A COHERENT, TUNABLE, FIR SOURCE

J.H. Brownell, M.F. Kimmitt, J.C. Swartz and J.E. Walsh
Department of Physics and Astronomy, Dartmouth College, Hanover, New Hampshire 03755-3528
(March 18, 1998)

A tunable coherent source which operates in the THz–FIR region of the spectrum has been developed. The device, termed a grating-coupled oscillator (GCO) uses the beam in a scanning electron microscope (SEM) and a diffraction grating placed in the e-beam's focal region to generate the radiation. Distributed feedback is provided by the grating itself and the e-beam is focused and positioned using the microscope's internal control system. A summary of operating characteristics of the present device and a survey of the scaling relations which will determine the spectral coverage is presented. Comments on what will be required in order to develop a very compact device are also included.

I. INTRODUCTION

The region of the electromagnetic spectrum which falls in the approximate band of wavelengths between 10 and 1000 μm, the so-called far-infrared (FIR) spectral region, is relatively devoid of tunable, coherent, radiation sources. Until quite recently, and relative to the range of options available at longer and shorter wavelengths, this assertion would be almost indisputable. However, the challenge presented by the lack of sources together with the existence of a broad range of interesting research puzzles and opportunities has led to a renewed interest in providing access to this spectral region. The present note deals with one promising approach to a means of producing tunable THz or FIR radiation.

The beam in a scanning electron microscope (SEM) and a diffraction grating mounted in the e-beam focal region has been used to produce coherent radiation [1] over a range of wavelengths that extends from approximately 250 μm out to 1000 μm. Termed a grating-coupled oscillator (GCO), the device is a new variation on an old theme.

Observation of radiation produced by electrons skimming over a diffraction grating was first reported by Smith and Purcell [2] in 1953. Even earlier, Salisbury had filed a patent application [3] on a device based on the coupling of moving electrons and a diffraction grating although Salisbury apparently did not conduct experiments until somewhat later [4]. Others [5–8] have also followed up on the early work.

The radiation mechanism described in reference [1], which has become associated with the authors' names, was essentially an incoherent or shot noise process. Individual rulings on the grating contributed coherently to the passage of a single electron but the contributions of each electron in the beam added incoherently. This was a consequence of the fact that in the early experiments, the focus was on short wavelengths, visible, and the size of the beam was large relative to the wavelength. The relative beam energy which is also a factor in the dimensionless coupling parameter was also low. A quantitative discussion of this point is presented further along in the manuscript.

Coherent radiation at mm [9–12] and sub-mm [13,14] wavelengths has been introduced in grating-coupled devices. Termed either Orotrons [9,11–14] or the Ledatron [10], these devices used gratings embedded in Fabry-Perot resonators and electron beam technology similar to that used in other microwave tubes to produce the radiation. The name Ledatron, introduced by Mizuno [10], was an acronym that was chosen in order to emphasize the dual nature of the surface modes and the importance of both the bound and radiative space harmonics in the coupling and emission process.

In the present device it is the distributed feedback on the grating itself that leads to bunching of the electron beam and the growth of coherent radiation. The beam voltages are modest (10-50 kV) but higher than those used in any but high-power tubes. Beam current density is high (100 A/cm^2 or greater), but the total currents are modest (100's μA). The "quality" of the electron beam, energy spread and emittance are critical factors. Thus, overall, the "brightness" of the beam is very high. The "open" nature of the resonator together with the extremely bright electron beam are the essential features of the device.

The remainder of the paper is divided as follows: A survey of device performance will be given in Section II and a summary of basic scaling relations that govern device operation is contained in Section III. These sections are followed by brief remarks on possible means by which very compact GCO devices might be realized, and by concluding remarks.

II. SURVEY OF EXPERIMENTAL RESULTS

Given the importance of beam quality and brightness, an SEM is the ideal device for exploring the potential of the GCO. The beam quality is excellent and the microscope's own focusing and transport elements may be used to shape and position the beam. The beam column of the SEM used in the present experiments is illustrated in Fig. 1. Electrons are emitted from a Tungsten "hairpin" cathode and focussed by a Wehnelt electrode and a series of magnetic lenses. The waist of the beam is placed at approximately the midpoint of the grating and at present the lower limit to the waist diameter is approximately 25 μm. This however is a machine-design imposed but not an absolute limit. The beam may also be swept either in and out along the grating normal or across the grating surface. This provides a convenient temporal reference modulation. Operation in fixed spot temporally pulsed mode is also an option.

The grating is placed on a miniature "optical bench" which is mounted on the microscope stage. At present the FIR optical system limits observation to the normal direction and the grating parameters are chosen to optimize normal emission. Designs that circumvent this limitation are under evaluation.

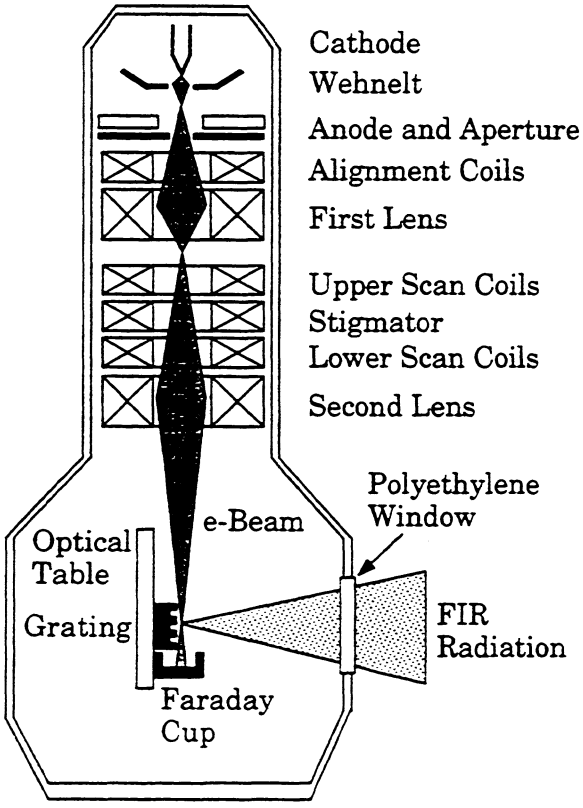

FIG. 1. Diagram of the SEM optical system.

A typical example of a plot of observed power versus electron beam current is shown in Fig. 2. It has two characteristic regions. When the current is relatively low and/or the beam diameter is comparatively large, the observed power increases linearly with current. This is characteristic of a shot noise or spontaneous emission process. In this region, a detailed analysis of the emission process has been carried out [15]. The emitted power in W/sr is given by:

$$\frac{dP}{d\Omega} = eI\frac{Nn^2}{2\ell\epsilon_0}F\,|R_n|^2\exp\left(-x_0/\lambda_e\right) \qquad (1)$$

where e is the electron charge, I is the beam current, N is the number of grating periods, n is the order of emission, ℓ is the grating period, and ϵ_0 is he permittivity of free space. Other parameter which appear in Eq. (1) are:

$$F = \frac{\sin^2\theta}{\left(1/\beta - \cos\theta\right)^3} \qquad (2)$$

$$\lambda_e = \frac{\gamma\beta\lambda}{4\pi} = \frac{\gamma\beta\ell}{4\pi|n|}\left(\frac{1}{\beta} - \cos\theta\right) \qquad (3)$$

Eq. (2) is the variation of the emission with polar angle. The symbols β and γ are respectively the electron velocity relative to the speed of light and the relative electron energy. Angles are measured with respect to the electron beam axis and x_0 is the distance of the infinitessimally thick beam above the grating. When observed power is composed with the prediction of Eq. (1), the measured beam profile is folded together with the evanescent field length given by Eq. (3). The remaining factor in Eq. (1), $|R_n|^2$, is in effect an antenna gain and the notation is that first introduced by van den Berg [16]. A detailed discussion that is adapted to the conditions of this experiment may be found in Urata [17].

When evaluated for parameters used in producing Fig. 2 and assuming an interaction length of 5 mm, Eq. (1) would predict emitted power levels of the order of 100 pW/μA-sr. The effective field of view of the collection optics is approximately 0.07 sr. The FIR emission is detected with a silicon composite bolometer placed between 0.5 and 1.0 m distant from the grating. Although the loss in the collection system is not accurately known, the theoretical predictions and estimated geometrical factors are consistent with the sub-nW power levels observed in the range where $P \propto I$.

The focused beam will support fast and slow space charge modes. As the beam plasma frequency is increased, those modes become resolved on the scale

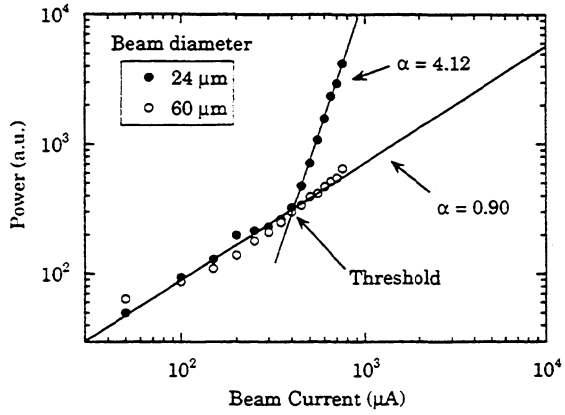

FIG. 2. Detected power vs. beam current. Fits of the form $y = Ax^{\alpha}$ are shown for the linear and superlinear regimes.

of the free spectral range which is determined by the beam velocity and the interaction length (i.e. the transit time). When, by increasing the beam current, this regime is reached, it is expected that coupling of the "negative energy" slow space charge wave with a co-propagating space harmonic component could result in a bunching of the beam. In this case, growth of the component of the emitted radiation will occur. While the details of the theory in this regime are still under development, such a transition is indeed observed. The transition occurs when the beam plasma frequency times the transit time exceeds 0.2-0.25. Beyond the transition point, the radiated power grows rapidly as a power of the current exceeding the expected spontaneous emission by 1 to 2 orders of magnitude. The exponent in this power law relation typically ranges from 3 to 6 and is sensitive to the operating conditions. With the present operating parameters, the system does not appear to have reached saturation.

It is clear that the finite length grating is functioning as a relatively high quality surface resonator but the details are yet to be understood. A similar caveat applies to the non-linear regime but Eq. (1) provides a basis for some interesting estimated. Since it is proportional to the product of the electron charge and the current, it has the characteristic form of a shot noise formula. If it is multiplied and divided by a spectral interval, $d\omega$, and the product eI factored out, what remains is a "radiation resistance". The spectral width of the spontaneous emission "Smith-Purcell line" has been deduced from both grating spectrometer and Fourier transform interferometer measurements. In either case the spectral width is about $\Delta\nu \approx 1\text{cm}^{-1}$. Converting this to an angular frequency, $d\omega$, and using a beam current of 100 μA, the factors

$$eId\omega = 3.2p\text{W}/\Omega \qquad (4)$$

Thus the measured power near the upper limit of the spontaneous emission regime indicates that the radiation resistance lies between 1 and 10 kΩ. The interaction length and the exact value of the beam profile – evanescent wave overlap are not determined precisely. However the 1–10 kΩ range for a radiation resistance is also consistant with an independent evaluation of Eq. (1) (after factoring out eI and evaluating $d\Omega/d\omega$).

A bunched beam with 100 μA rms current would be expected to generate between 10 and 100 μW. A beam with approximately one order of magnitude greater current ($\approx$ 1 mA) would produce power levels in the mW range.

These arguments are qualitative but they are also based on fundamental constraints. The estimates probably represent reasonable upper limits to what can be expected from SEM electron optical system based e-beam technology.

III. SCALING OF GCO DESIGN CONSTRAINTS

A discussion of the constraints governing GCO operation is facilitated by first examining the dispersion plane associated with the electromagnetic fields above a grating. A schematic dispersion plane is illustrated in Fig. 3. The vertical axis is the angular frequency measured in units of 2π times the speed of light divided by the grating period. The horizontal axis is the wave number along the grating in a direction perpendicular to the rulings. Again, the units are normalized.

The plane is divided into two principal regions, "fast" and "slow". These designations are relative to

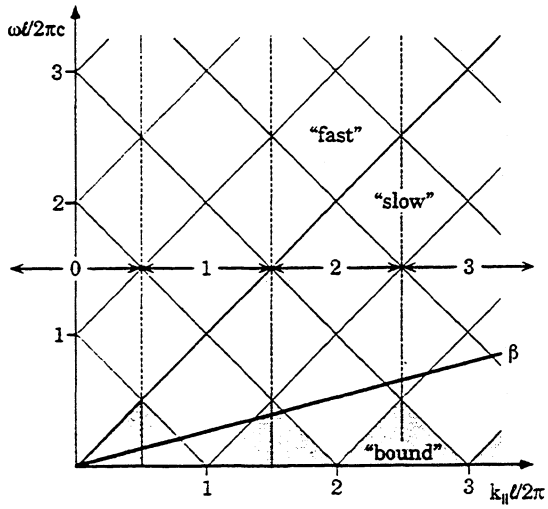

FIG. 3. Schematic of GCO dispersion plane.

the speed of light, the lines with slope ± 1 on the diagram. Each Fourier component of the field above the grating will contain a complete set of space harmonic whose axial wave numbers differ by $2\pi/\ell$. Space harmonics with phase velocities that fall within the "light cone", the region labeled fast, satisfy radiative boundary conditions. The points in the fast region represent components of either incident and scattered waves or an outgoing wave generated by the beam.

Points on the plane which fall outside the light cone have phase velocities less than the speed of light. Space harmonic components in this region are non-radiative but they do serve as a coupling mechanism for the electron beam. A "beam line" is also shown on the figure. Along this line the relation

$$\omega = k_{\|} v \tag{5}$$

is satisifed (ω is the angular frequency, $k_{\|}$ is the axial wave number in dimensional units, and v is the velocity of the beam. In the current discussion only waves which have at least one space harmonic component in this light cone are of interest. Thus, the darker shaded areas, marked bound, may be ignored. The wavenumber which appears in Eq. (5) may be broken down into two components

$$k_{\|} = k_0 + 2\pi |n|/\ell \tag{6}$$

where

$$k_0 = (\omega/c)\cos\theta \tag{7}$$

is the axial component of the wavenumber along the grating that would be associated with an outgoing radiative wave. Combining Eqs. (5 – 7) and choosing $|n| = 1$ yields

$$\frac{\omega}{c} = \frac{2\pi/\ell}{1/\beta - \cos\theta} \tag{8}$$

or

$$\lambda = \ell\,(1/\beta - \cos\theta) \tag{9}$$

which is the well-known relation discussed by Smith and Purcell in Ref. [2]. It can also be deduced using the Huygens construction.

The choice $|n| = 1$ is not necessarily the dominant mode. It is interesting to note that if, for instance, the depth of the grating is chosen in order to optimize the spontaneous emission for $|n| = 3$ that mode will also dominate above threshhold (Fig. 4). Small variations in voltage will also lead to $|n| = 1$ and $|n| = 3$ operating simultaneously (Figs. 5 and 6). The potential for operation on higher-order modes of the grating provides an important degree of freedom for grating design.

Another important constraint is related to the evanescent scale length of the slow space harmonics. Outside the light cone, the square of the perpendicular component of the total wavenumber is less than

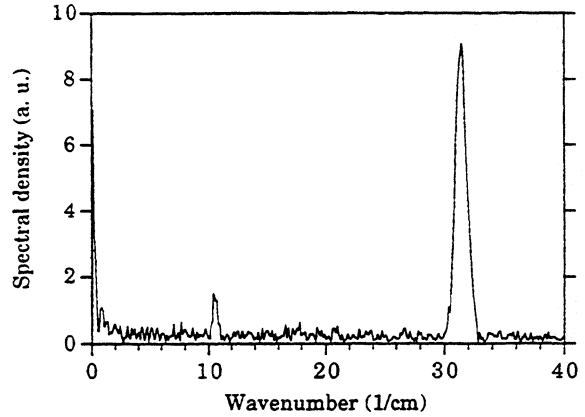

FIG. 4. Power spectrum of GCO operating at $|n| = 3$.

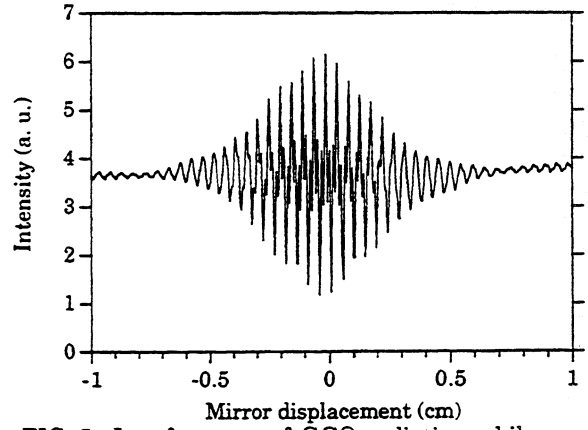

FIG. 5. Interferogram of GCO radiation while operating simultaneously at $|n| = 1$ and $|n| = 3$.

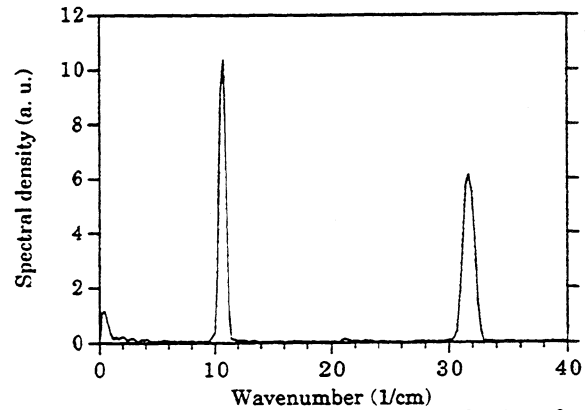

FIG. 6. Power spectrum inferred from the interferogram in Fig. 5.

zero and the wavenumber itself is pure imaginary and has a magnitude

$$|k_\perp| = \sqrt{k_\parallel^2 - \omega^2/c^2} \tag{10}$$

Since energy transfer is through the nearly-synchronous co-propagating space harmonic the relation $k_\parallel = \omega/v$ can be used to infer that

$$|k_\perp| = \omega/v\gamma \tag{11}$$

where $\gamma = 1/\sqrt{1-\beta^2}$. Thus,

$$|k_\perp| = 2\pi/\gamma\beta\lambda \tag{12}$$

or

$$|k_\perp|^{-1} = \lambda_e \tag{13}$$

the evanescent scale length introduced in Section II. In general, good coupling will require the beam diameter to be

$$d \leq \lambda_e \tag{14}$$

or

$$\lambda \geq 2\pi d/\gamma\beta \tag{15}$$

Using the values associated with a 25 kV beam gives the relation

$$\lambda \geq 20d \tag{16}$$

Good coupling at 300 μm (1 THz) would be achieved with a beam parameter of the order of 15 μm. This is consistent with data obtained in the proof-of-principle experiments. Experiments designed to test the lower limits of d are currently in progress. Much smaller values of d are achievable and operation well above 1 THz may be expected. Further extension of the evanescence scale length may also be achieved by increasing the beam voltage.

A final pair of scaling relations follow if it may be assumed that the depth of field of the beam focus is emittance dominated and that this limits the effective interaction length. In this case the interaction length L is related to the beam diameter by the expression

$$L \simeq \frac{\gamma\beta d^2}{\epsilon_N} \tag{17}$$

where ϵ_N is the normalized emittance. Since d and λ_e are comparable, the relation

$$L \simeq \frac{\gamma\beta\lambda_e^2}{\epsilon_N} \tag{18}$$

also follows.

Threshhold occurs when the beam plasma frequency ω_b times the transit time of a beam electron through the interaction length exceeds about 0.25. Operation well above threshhold will require

$$\frac{\omega_b L}{\gamma^{3/2} v} > 1 \tag{19}$$

(where the factor $\gamma^{3/2}$ has been included since the bunching is longitudinal; it has, of course, a negligible numerical effect for non-relativistic beams).

With the aid of the usual expression for the beam plasma frequency and multiplying and dividing by additional factor of beam velocity yields the constraint

$$\frac{JL^2}{(\epsilon_0 mc^3/e)(\gamma\beta)^3} > 1 \tag{20}$$

where J is the beam current density. If the relation between the interaction length and the evanescent scale are invoked, the constraint becomes

$$\frac{J\lambda_e^4}{(\epsilon_0 mc^3/e)\gamma\beta\epsilon_N^2} > 1 \tag{21}$$

Finally, if re-written in terms of wavelength, the result

$$\lambda > 2\pi \left[\frac{(\epsilon_0 mc^3/e)\epsilon_N^2}{(\gamma\beta)^3 J}\right]^{1/4} \tag{22}$$

is obtained. Evaluating this last expression using typical parameters for the present electron optical system indicates that we are operating near the lower wavelength limit of that apparatus.

IV. TOWARD A COMPACT GCO

The GCO described in the preceding sections is already compact by some standards. As is evident from the scaling relations discussed in Section III, increase of beam energy as well as a decrease of beam emittance can be used to lower the limiting wavelength. Increasing the beam energy is, of course, the route taken in relativistic electron-beam-driven, free-electron lasers (FEL). The present GCO is already far smaller than these devices. The GCO's output power is much smaller than the levels produced by a relativistic beam-driven FEL. However, it is already sufficient for application in spectroscopy or as a local oscillator.

Straightforward engineering and elimination of the non-essential features of the SEM would lead immediately to a much smaller device. It is also interesting to speculate on more dramatic options.

The beam voltage required for GCO operation probably need never exceed 50 kV and in the present device, THz operation is achieved with only 20 kV of beam voltage. This range is well within the scope of modern dc–dc converter-based power supply technology. The beam currents required are also modest and well within the scope of current converter-based power supplies. These supplies can now be obtained in very compact packages.

A second major reduction in size might be obtained if modern field emission cathode technology were employed. The primary motivation for much work on the field emission cathode is for use in flat panel displays. However, use in microwave tubes has also been a factor. The GCO is an ideal place to use this technique. A ribbon beam a micron thick and about a millimeter wide propagating a distance no more than a few centimeters would be ideal. Power consumption and heat load would be reduced dramatically.

The GCO is also a linear device and standard energy recovery technology is probably applicable. Implementation of energy recovery would improve terminal efficiency. If done in a way such as to also reduce beam intercept at high voltages the already-modest x-ray production could be further reduced.

Finally, although the grating is a simple and reliable means of converting electron beam kinetic energy to coherent radiation, other photonic band gap structures might be employed. The present GCO uses only the distributed feedback on the grating. More complex structures, particularly ones with well-defined high-quality factor modes, may offer significant advantages.

V. CONCLUSIONS

A potentially very useful THz-FIR source has been developed. Based on a novel variation of an old theme, the device is simple and versatile. Power output levels and tuning range are already of interest in some applications and fundamental scaling arguments support the claim that considerable extension of the tuning range and output power is possible. If operated near the limit of established electron beam optical art it will be possible to access the challenging 10-1000 μm wavelength range.

Support from ARO Contract DAAH04-95-1-0640, DoD/AF DURIP Contract F49620-97-1-0287, and Vermont Photonics, Inc., is gratefully acknowledged.

[1] J. Urata, M. Goldstein, M.F. Kimmitt, A. Naumov, C. Platt and J.E. Walsh, Phys. Rev. Lett. **80**, 516 (1998).
[2] S.J. Smith and E.M. Purcell, Phys. Rev. **92**, 1069 (1953).
[3] W.W. Salisbury, US Patent 2,634,372, filed October 26, 1949, granted April 7, 1953.
[4] J.P. Bachheimer, Phys.Rev. B **6**, 2985 (1972).
[5] W.W. Salisbury, Science **154**, 386 (1966).
[6] E.L. Burdette and G. Hughes, Phys. Rev. A **14**, 1766 (1976).
[7] A. Gover, P. Dvorkis and U. Elisha, J. Opt. Soc. Am. B **1**, 723 (1984).
[8] I. Shih, D.B. Chang, J.E. Drummond, K.L. Dubbs, D.L. Masters, R.M. Prohaska and W.W. Salisbury, J. Opt. Soc. Am. B **7**, 351 (1990).
[9] F.S. Rusin and G. Bogomolov, Proc. IEEE **57**, 720 (1969).
[10] K. Mizuno and S. Ono, The Ledatron, Infrared and Millimeter Waves 1: Sources of Radiation, ed. K. Button (Academic Press, Inc., 1979), Ch. 5, pp. 213-233.
[11] D.E. Wortman, H. Dropkin and R.P. Leavitt, IEEE Journ. Quant. Elect. QE-17(8), 1341 (1981).
[12] V.P. Shestapolov, Diffraction Electronics (Kharkhov: 1976).
[13] E.J. Price, Appl. Phys. Lett. **61**, 252 (1992).
[14] J.H. Killoran, IEEE Trans. Pl. Sci. **22**, 530 (1994).
[15] M. Goldstein, J.E. Walsh, M.F. Kimmitt, J. Urata and C.L. Platt, Appl. Phys. Lett. 71, 452 (1997) and A Far-Infrared Smith-Purcell Micro-Radiator, Ph.D. thesis, 1994, available from Department of Physics and Astronomy, Dartmouth College, Hanover, NH 03755.
[16] P.M. van den Berg, J. Opt. Soc. **63**, 1588 (1973).
[17] J. Urata, Spontaneous and Stimulated Smith-Purcell Radiation Experiments in the Far-Infrared, Ph.D. thesis, 1997, pp. 19-20, available from Department of Physics and Astronomy, Dartmouth College, Hanover, NH 03755.